Materials Science & Engineering A 678 (2016) 243–251

Contents lists available at ScienceDirect

Materials Science & Engineering A

journal homepage: www.elsevier.com/locate/msea

Microstructure evolution and room temperature fracture toughness of directionally solidified NiAl–31Cr3Mo–0.2Si near-eutectic alloy at different withdrawal rates

Huan Liu, Weidong Xuan*, Xinliang Xie, Jianbo Yu, Jiang Wang, Zhongming Ren*

State Key Laboratory of Advanced Special Steel, Shanghai University, Shanghai 200072, PR China

ARTICLE INFO

Keywords:
NiAl intermetallics
Directional solidification
Microstructure
Fracture toughness

ABSTRACT

The microstructure evolution and room temperature fracture toughness of directionally solidified NiAl–31Cr3Mo–0.2Si (at%) near-eutectic alloy at different withdrawal rates were investigated. The results showed that NiAl dendrites were eliminated and fully eutectic structure was achieved by applying appropriate withdrawal rates. The microstructure evolved from planar eutectic to primary NiAl dendrites + cellular eutectic and then to dendritic eutectic with the increasing withdrawal rate. Correspondingly, the interlamellar spacing and cell size decreased gradually. The relationship between eutectic interlamellar spacing with withdrawal rate can be summarized as $\lambda = 4.74V^{-0.38}$. The fracture toughness of alloys with fully eutectic structure was much higher than that of alloys with NiAl dendrites. It increased up to 2.5 times. The high fracture toughness may be attributed to some toughening mechanisms, such as crack bridging, crack deflection, interface debonding and microcrack linkage. The existence of primary dendrites would seriously deteriorate the fracture toughness.

1. Introduction

The ordered intermetallic compound NiAl exhibits high melting point, relatively low density, high thermal conductivity and excellent high temperature oxidation resistance compared to conventional Ni-based superalloys, which make it an attractive candidate for the next generation of high temperature structural materials [1–3]. However, the poor ductility at room temperature and low creep resistance at elevated temperature limit its industrial application [4,5]. Over the past decades, many research have been proceeded to enhance the room temperature facture toughness and elevated temperature strength, such as alloying of additions [6,7], particulate reinforced composites [8,9] and directionally solidified eutectic composites [10–14]. In particular, directionally solidified NiAl–Cr(Mo) in-situ eutectic composite with a lamellar structure has been regarded as the most promising NiAl alloy for high temperature structural use [12].

Directionally solidified NiAl–Cr(Mo) eutectic composite has been researched widely since the 1970s, it exhibits a better combination of room temperature toughness and elevated temperature strength compared to other NiAl alloys. The facture toughness at room temperature of directionally solidified NiAl–28Cr6Mo eutectic alloy can reach 24.1 MPa$\sqrt{m}$ [12] and the tensile strength of directionally solidified NiAl–31Cr3Mo eutectic alloy can reach 348 MPa at 1093 °C [4]. Traditional Bridgman process combined with investment casting shell molds is widely used in industrial production of turbine blades. However, due to the high melting point of NiAl alloys, chemical reaction between melt and shell molds is inevitable, especially with the SiO_2 in shell molds [15–17]. In this case, Si impurities would be mixed into the alloy. Whittenberger et al. [18,19] had investigated the effects of minor alloying additions on the microstructure and mechanical properties of NiAl–31Cr3Mo. It was found that the small addition of Si introduced NiAl dendrites and decreased the toughness. Bogner et al. [20] also observed NiAl dendrites in NiAl–Mo eutectic alloy directionally solidified using an industrial scale Bridgman furnace. Above research indicated that the addition of Si in NiAl–Cr(Mo) eutectic alloy would introduce NiAl dendrites which seriously damaged the mechanical properties.

According to the coupled growth theory [21], fully eutectic structure can be achieved not only from eutectic alloys but also from near-eutectic alloys by adjusting the solidification parameters. Shang et al. [22,23] investigated the microstructure evolution of directionally solidified NiAl–Cr(Mo) hypereutectic alloys. They obtained fully eutectic structure with higher volume fraction of lamellar Cr(Mo) phase compared to the eutectic alloy. So far, little work was carried out on NiAl–Cr(Mo) eutectic alloys with Si addition. If the primary dendrites can be eliminated in NiAl–Cr(Mo) alloy with Si addition, the influence

* Corresponding authors.
E-mail addresses: wdxuan@shu.edu.cn (W. Xuan), renzm2201@163.com (Z. Ren).

http://dx.doi.org/10.1016/j.msea.2016.10.002
Received 20 July 2016; Received in revised form 28 September 2016; Accepted 3 October 2016
Available online 04 October 2016

of reaction between the melt and shell mold may be minimized. So NiAl–31Cr3Mo–0.2Si alloy which has the similar Si content with alloys solidified in shell molds [16] was adopted in present study, expecting to get fully eutectic structure and better properties by controlling the withdrawal rate. In this paper, we investigated the microstructure evolution and room temperature fracture toughness of directionally solidified NiAl–31Cr3Mo–0.2Si near-eutectic alloy at different withdrawal rates.

2. Experimental procedures

The Ni–33Al–31Cr–3Mo–0.2Si (at%) alloys used in this study were prepared in a vacuum induction melting furnace. Cast samples were cut and enveloped in high-purity corundum tubes with an inner diameter of 10 mm and a length of 200 mm for the directional solidification. The experimental apparatus, which is shown in Ref. [24], consists of a Bridgman-Stockbarger-type furnace, a pulling system and a temperature controller. A water-cooled cylinder containing liquid Ga–In–Sn metal was used to cool down the sample. The temperature gradient in front of the solid/liquid interface was controlled by adjusting the temperature of hot zone, which was insulated from the water-cooled cylinder by a refractory disc. The specimens were heated up to 1600 °C and pulled down at the withdrawal rates of 1, 2, 5, 10, 25, 50, 100 and 200 μm/s, respectively. To observe the morphology of solid/liquid interface, the samples were quickly quenched into the liquid metal after stable growth for more than 60 mm. The temperature gradient in present study was 90 K/cm.

The directionally solidified samples were cut along the longitudinal and transverse directions. After grinding and polishing, the specimens were etched with a solution of 80% HCl + 20% HNO_3 by volume. The microstructures were observed by an optical microscope and a scanning electron microscopy (SEM, FEI Quanta 450) equipped with an energy dispersive spectroscopy (EDS, EDAX Octane Plus). The interlamellar spacing was measured by Image Pro Plus metallurgical analysis software.

Room temperature fracture toughness of the alloys was measured using three-point bending test. The bend bars were 30×6×3 mm in size with a narrow straight 3 mm-deep notch. The bars were taken from the steady-state growth region by wire electro-discharge machining (EDM) with the length direction parallel to the growth axis. The tests were performed in air at room temperature in a DNS100 universal test machine. The cross-head speed was 0.05 mm/min for the three-point bending test.

3. Results and discussion

3.1. Microstructure evolution

Fig. 1 shows the microstructure of as-cast alloy. The microstructure was consisted of equiaxed dendrites and lamellar eutectic. The dendrites were identified as NiAl phase by EDS. None of other phases was found in the alloy. Fig. 2 shows the solid/liquid interface morphologies of directionally solidified NiAl-31Cr3Mo-0.2Si near-eutectic alloy grown at 1, 2, 5, 10, 25, 50, 100 and 200 μm/s, respectively. It can be observed that the primary NiAl dendrites were only existed when the withdrawal rates was 5 and 10 μm/s. In samples grown slower or faster than the speeds, the primary dendrites disappeared. Moreover, as the withdrawal rate increasing, the eutectic morphology changed from planar eutectic to cellular eutectic and then to dendritic eutectic.

The steady-state transverse microstructures of directionally solidified NiAl–31Cr3Mo–0.2Si near-eutectic alloy grown at different withdrawal rates are shown in Fig. 3. When the withdrawal rates were 1 and 2 μm/s, the transverse microstructure were fully lamellar eutectic without any primary dendrites. The eutectic microstructure consisted of alternating NiAl phase (gray plates) and Cr(Mo) phase (light plates).

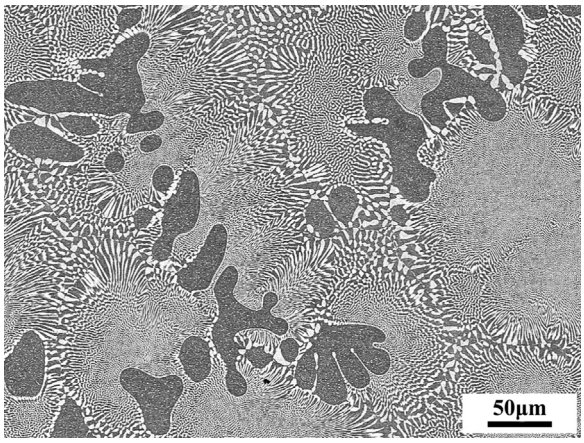

Fig. 1. Microstructure of as-cast NiAl–31Cr3Mo–0.2Si near-eutectic alloy.

When the withdrawal rates increased to 5 and 10 μm/s, primary dendrites were observed. Furthermore, from the magnified images, we can see obviously that the eutectic morphology changed to cellular. NiAl and Cr(Mo) phases exhibited a radially emanating pattern from the cell interior to its boundaries. The NiAl and Cr(Mo) plates were fine near the cell center and much coarser at the intercellular zone. When the withdrawal rates were even higher, the morphologies evolved to two-phase dendritic eutectic, and the primary NiAl dendrites disappeared again. The transverse structure of dendritic eutectic was similar to cellular eutectic, except that some small cells were contained in a eutectic cluster. The small cells were actually dendrite arms of eutectic dendrites. As the withdrawal rate increased, the size of eutectic cells decreased.

The interlamellar spacing of NiAl–31Cr3Mo–0.2Si near-eutectic alloys grown at different withdrawal rates is shown in Fig. 4. It can be observed that the interlamellar spacing decreased with increasing withdrawal rate. When the withdrawal rate increased from 1 to 200 μm/s, the interlamellar spacing decreased from 4.74 to 0.53 μm. A power-law fitting to the data resulted in the following equation:

$$\lambda = 4.74V^{-0.38} \quad (1)$$

where λ is the interlamellar spacing and V is the withdrawal rate. The relationship between the interlamellar spacing and withdrawal rate coincides with J-H model [25] for planar binary eutectic: $\lambda^2 V$ = constant, which also indicates that the model may extend to cellular and dendritic eutectic structure.

The existence of primary dendrites indicated that the addition of Si may change the eutectic composition, resulting in the alloy composition deviated from the eutectic point. To study the distribution of element Si, the average composition of NiAl and Cr(Mo) phases was measured at more than 10 positions by EDS. The EDS spectrums and composition of the two eutectic phases are shown in Fig. 5 and Table 1, respectively. We can see that all the Si was dissolved in Cr(Mo) phases. The solution of Si will decrease the liquidus of Cr(Mo) phase, then the intersection of the two liquidus (i.e. eutectic point) shifts toward the Cr(Mo) phase. For alloy deviated from the eutectic point, the liquidus is always higher than eutectic temperature based on equilibrium phase diagram. Accordingly, the primary phase has larger undercooling and tends to grow faster than eutectic, which is known as single-phase instability, as shown in Fig. 6(a1) [26]. However, due to the different growth characteristics of dendrite and eutectic, the growth speed of diffusion-coupled eutectic is usually faster than isolated dendrite near the eutectic composition. Therefore, the eutectic may outgrow the individual dendrites, and fully eutectic structure is obtained in off-eutectic alloy. Jackson [27] was the first to propose a theoretical model for competitive growth between the primary dendrite and composite structure. Burden and Hunt [28] then modified the model. According to the theory, whether the morphology is fully eutectic or primary